

DOI: 10.1002/ange.200504354

**Control over Electron Transfer in Tetrathiafulvalene-Modified Single-Walled Carbon Nanotubes\*\****M. Ángeles Herranz, Nazario Martín,\*  
Stéphane Campidelli, Maurizio Prato,\* Georg Brehm,  
and Dirk M. Guldi\**

Fullerenes and, more recently, carbon nanotubes (CNTs) have emerged as an innovative and new class of nanoscale carbon-based materials that are currently under intensive investigation.<sup>[1]</sup> The excitement in this area is, by large, a consequence of their promising functions in molecular-scale electronic applications. In stark contrast to the wealth of [60]fullerene-based donor–acceptor dyads studied so far,<sup>[2]</sup> the incorporation of single-walled carbon nanotubes (SWNTs) into donor–acceptor ensembles has been scarcely explored, and only a few examples involving the covalent linkage of electroactive species are known.<sup>[3]</sup> For example, some of us reported the functionalization of SWNTs with electron-donating ferrocene and confirmed that in this particular case electron transfer occurred from the ferrocene to the photoexcited SWNT. This initial work stimulated the use of SWNT nanoconjugates in solar energy conversion applications.<sup>[4]</sup> However, control over the electron transfer in SWNTs remains a central but unsolved topic.

[\*] Dr. M. Á. Herranz, Prof. Dr. N. Martín  
Departamento de Química Orgánica  
Facultad de Química  
Universidad Complutense  
28040 Madrid (Spain)  
Fax: (+34) 91-394-4103  
E-mail: nazmar@quim.ucm.es

Dr. S. Campidelli, Prof. Dr. M. Prato  
Dipartimento di Scienze Farmaceutiche  
Università di Trieste  
Piazzale Europa, 1, 34127 Trieste (Italy)  
Fax: (+39) 040-52-572  
E-mail: prato@unis.it

Dr. G. Brehm, Prof. Dr. D. M. Guldi  
Friedrich-Alexander-Universität Erlangen-Nürnberg  
Institute for Physical Chemistry  
Egerlandstrasse 3, 91058 Erlangen (Germany)  
Fax: (+49) 9131-852-8307  
E-mail: dirk.guldi@chemie.uni-erlangen.de

[\*\*] This work was supported by the MEC of Spain (project CTQ2005-02609/BQU), the CAM (project P-PPQ-000225-0505), the UCM (project PR1/05), the European Union (TRN network WONDER-FULL), the MIUR (PRIN 2004, no. 2004035502), the Deutsche Forschungs-gemeinschaft (SFB 583), FCI, and the Office of Basic Energy Sciences of the US Department of Energy (NDRL no. 4661). We thank Christian Ehli and G. M. Aminur Rahman for their useful discussions. M.A.H. would like to acknowledge the CICYT for a “Ramón y Cajal” contract.



Supporting information for this article is available on the WWW under <http://www.angewandte.org> or from the author.

Herein, we focus on the first series of structurally well-defined and electronically fine-tuned donor–acceptor SWNT nanoconjugates, in which tetrathiafulvalene (TTF) and/or  $\pi$ -extended tetrathiafulvalene (exTTF) are integrated as electron donors. Previous studies have illustrated the remarkable and numerous benefits of utilizing TTF or exTTF in electron-transfer events.<sup>[5]</sup> Here we provide, for the first time, a complete spectroscopic characterization of charge-separation products in photoexcited TTF–SWNT and exTTF–SWNT conjugates, that is, the generation of reduced and oxidized components, and a kinetic analysis that documents the successful control over the charge recombination processes by structural variation.

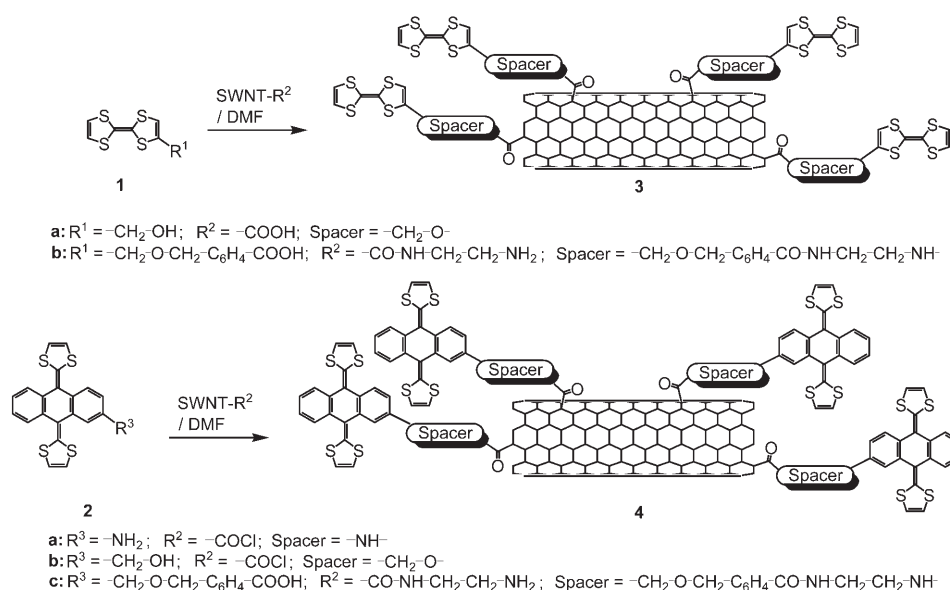
In our strategy, the as-prepared HIPco SWNTs were purified, shortened, and modified with carboxylic groups by treatment with  $\text{HNO}_3$  and  $\text{H}_2\text{SO}_4/\text{H}_2\text{O}_2$  (Scheme 1).<sup>[6]</sup> Compound **3a** was obtained by an esterification reaction between

functionalities in the SWNT nanoconjugates (**3a,b** and **4a–c**). Although some of the characteristic van Hove singularities of the SWNTs are observed in the near-infrared region of the absorption spectra (see the Supporting Information), the TTF and exTTF features—predominantly in the visible range—are nearly entirely masked. The Raman spectra, on the other hand, of all the SWNT samples (SWNT–COOH, SWNT–TTF **3a,b**, SWNT–exTTF **4a–c**) reveal intense disorder bands (D band) prior to and after the condensation reaction. However, a decrease in the relative intensities, using the G band as internal reference, of these bands was observed upon condensation (see the Supporting Information). This behavior has previously been observed in some related systems.<sup>[10]</sup> In addition, the G band is noticeably downfield shifted in the spectra of the donor–acceptor nanoconjugates (**3a,b** and **4a–c**) relative to that seen in the reference SWNT. This observation is consistent with studies of charge-transfer reactions of SWNTs doped with either donor or acceptor groups.<sup>[11]</sup>

The functionalization of the nanotubes has also been investigated by TGA under nitrogen. Both SWNT–COOH and SWNT–CONHCH<sub>2</sub>CH<sub>2</sub>NH<sub>2</sub> present a weight loss of about 23 % between 200 and 600 °C which corresponds to the destruction of the organic groups present on the surface of the nanotubes. The functionalized nanotubes **3a,b** and **4a–c** exhibit a weight loss of about 27–34 % in the same temperature range (see the Supporting Information). Thus the TGA results indicate that the SWNT–TTF and SWNT–exTTF nanoconjugates all show a similar behavior upon heating. As expected, the increased weight loss compared to their respective precursors stems from the covalent linkage of the TTF/exTTF moieties to the sidewalls of the nanotubes.

The presence of SWNTs in all the studied samples was corroborated by means of TEM and AFM (a representative TEM picture is shown in the Supporting Information).

SWNTs are present as aggregates of several micrometers length and also as small bundles with diameters of 20 to 50 nm, in which very thin bundles or individual tubes can be seen at the edges. These characteristics are fundamentally different from those of the starting HIPco SWNTs (www.cnanotech.com), which exhibit thick and long bundles exclusively. Complementary AFM investigations (Figure 1) permitted a more detailed insight into the SWNT–TTF and SWNT–exTTF nanoconjugates. The samples were prepared by spin coating solutions of SWNT–TTF and SWNT–exTTF in DMF on to silicon wafers. This technique allowed us to visualize very thin bundles (several hundreds of nanometers long and 3 to 10 nm in diameter) as well as individual tubes (100–500 nm long and 1.2–1.7 nm in diameter).



**Scheme 1.** Synthesis of TTF- and exTTF-functionalized SWNTs.

the short SWNT containing carboxylic acid groups and hydroxymethyl-substituted TTF (**1a**)<sup>[7]</sup> in the presence of 3-(3-dimethylaminopropyl)-1-ethylcarbodiimide (EDC) and 1-hydroxy-1*H*-benzotriazole (HOBt). For the synthesis of compounds **4a,b**, suitably functionalized short SWNTs (SWNT–COOH) were first treated with thionyl chloride to generate the respective acyl chloride functionalities and then treated with amine **2a**<sup>[8]</sup> or alcohol **2b**.<sup>[8]</sup> The TTF–SWNT and exTTF–SWNT nanoconjugates **3b** and **4c**, respectively, were obtained upon esterification of the corresponding carboxylic acids (**1b** and **2c**)<sup>[9]</sup> with short SWNTs, previously treated with ethylenediamine, in the presence of EDC and HOBt (see the Supporting Information for experimental details).

Compounds **3a,b** and **4a–c** were fully characterized by standard analytical and spectroscopic techniques such as FTIR, Raman, UV/Vis, thermogravimetric analysis (TGA), transmission electron microscopy (TEM), and atomic force microscopy (AFM). Importantly, the recorded FTIR spectra reveal the characteristic fingerprints of the amide and/or ester

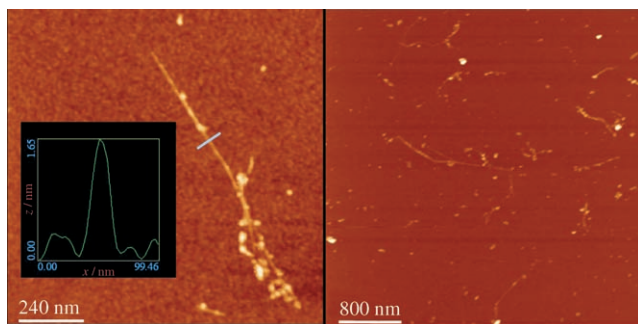


**Figure 1.** AFM images of SWNT-exTTF nanoconjugate **4a** on a silicon wafer. Right: a general view of the sample, left: a small aggregate of nanotubes.

The electrochemical properties of **3a,b** and **4a-c** were investigated in saturated solutions of DMF and THF containing 0.1 M  $n\text{Bu}_4\text{NClO}_4$  in an argon atmosphere. The voltammograms display a continuum of diffusion-controlled cathodic current, with an onset at around  $-0.4$  V, which is attributed (in accordance with previous studies<sup>[12]</sup>) to the reductive charging of the SWNTs. Single two-electron and chemically reversible oxidation processes are clearly discernible for derivatives **4a-c**. We assign them to exTTF-centered processes, even though they are positively shifted by approximately 100 mV relative to the reference systems **2a-c** (Figure 2). These shifts are likely a result of weak intramolecular electronic interactions between the electroactive units in the nanoconjugates. In sharp contrast, the characteristic two one-electron and chemically reversible oxidation steps of TTF in **3a,b** were observed as a broad peak, most probably involving both oxidation processes (see the Supporting Information). Based on the electrochemical data, the lowest energy levels of the  $(\text{SWNT})^--(\text{TTF})^+$  or  $(\text{SWNT})^--(\text{exTTF})^+$  conjugates are estimated to lie between 0.65 and 0.80 eV.

Notably, our approach towards dispersable donor-acceptor nanoconjugates preserves, although not entirely but at least in part, the electronic structure of the SWNTs.<sup>[13]</sup> The presence of the van Hove singularities in the near-

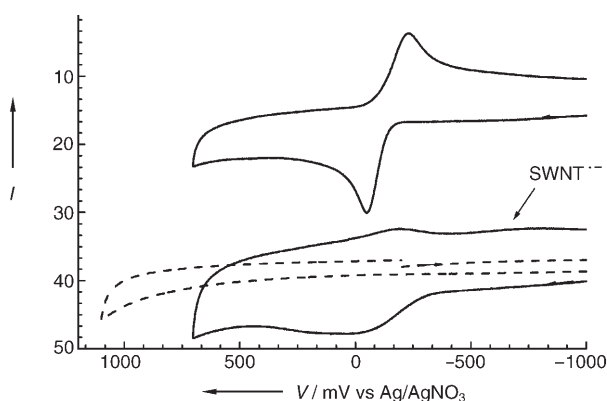


**Figure 2.** Cyclic voltammograms obtained for **2b** (0.5 mM; top) and **4b** (saturated solution, bottom) in a 0.1 M  $n\text{Bu}_4\text{NClO}_4$ /DMF solution. Sweep rate =  $500 \text{ mV s}^{-1}$ ,  $T = 25^\circ\text{C}$ , working electrode: glassy carbon, reference electrode:  $\text{Ag}/\text{AgNO}_3$ , and counter electrode: Pt wire. The dashed line corresponds to the background signal.

infrared region further supports this assumption. Consequently, near-infrared fluorescence spectroscopy emerges as a viable method to probe excited state interactions (that is, photoinduced charge separation) between photoexcited SWNTs (that is, with radiative lifetimes and nonradiative lifetimes as long as 3  $\mu\text{s}$  and 500 ps, respectively<sup>[14]</sup>) and the covalently linked donor moieties. An illustration is given in Figure 3, from which two important observations were deduced. Firstly, sets of fluorescence features are seen mirror imaged to the absorptive transitions. A likely rationale implies fluorescence from the semiconducting SWNTs. Secondly, a systematic quenching trend is discernable when comparing the fluorescence of the SWNTs with that of the SWNT-TTF or SWNT-exTTF conjugates. The quenching is significantly enhanced when shorter linkers are used to connect the TTF or exTTF units to the SWNTs.

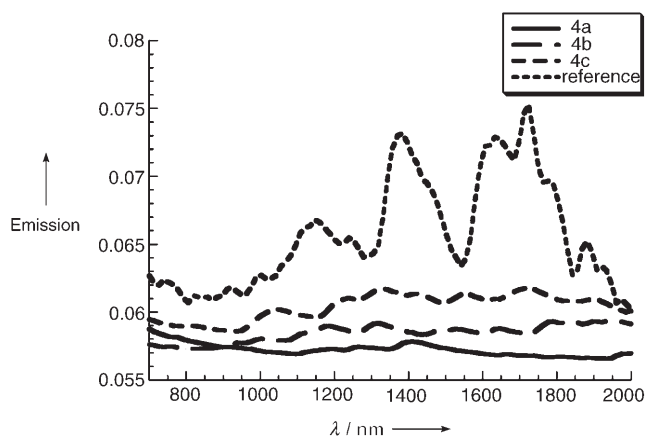


**Figure 3.** Near-infrared fluorescence of SWNT-COOH and SWNT-exTTF nanoconjugates **4a-c** with matching absorption at 600 nm.

Spectroscopic confirmation for the assumed charge separation came from transient absorption measurements performed with SWNT-COOH as well as the SWNT-TTF and SWNT-exTTF ensembles. Under the chosen conditions, laser excitation at 308, 337, or 355 nm, respectively, the reference conjugate SWNT-COOH in THF shows a fairly broad and long-lived transient species (see the Supporting Information). In stark contrast, nanosecond excitation of fine dispersions of SWNT-TTF and SWNT-exTTF in THF gave rise in the visible range (Figure 4) to the well-known signatures, namely, transitions at 440 nm and 660 nm, respectively, of the TTF and exTTF radical cations.<sup>[15]</sup> To gather evidence for the reduction of the SWNTs we examined the near-infrared region of the spectrum. In this region, the radical cation absorptions of the donor fragments are negligible and the van Hove singularities of the SWNTs constitute the major absorbing species. In fact, pulse radiolytic reduction experiments with aqueous suspensions of SWNTs, either in the form of a covalent nanoconjugate (SWNT-PSS) or noncovalent nanohybrid (SWNT/pyrene<sup>+</sup>), led to characteristic spectra.<sup>[16]</sup> The fact that we found such features in the present cases (Figure 4) lead us to postulate that the SWNTs are indeed reduced. In conclusion, the spectra recorded after nanosecond photolysis appear as

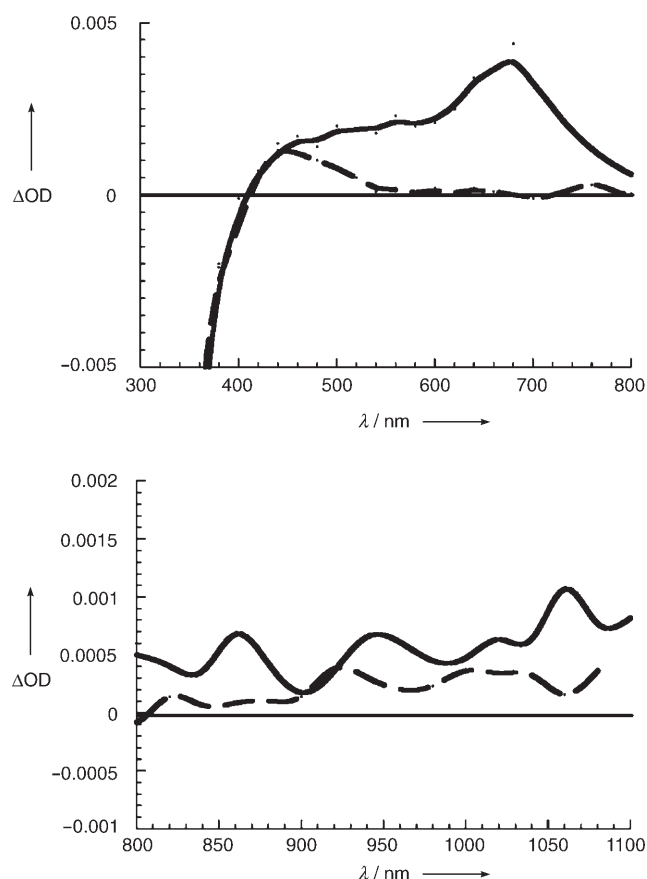


**Figure 4.** Differential absorption spectra (Vis: top and NIR: bottom) obtained upon nanosecond flash photolysis (532 nm) of **3b** (dashed line) and **4c** (solid line) in nitrogen-saturated THF solutions with a time delay of 150 ns.

composite spectra showing the attributes of the oxidized donor and the reduced acceptor components within the photoexcited SWNT-TTF or SWNT-exTTF nanoconjugates.<sup>[17]</sup>

Kinetic analysis of the different SWNT-TTF and SWNT-exTTF nanoconjugates allowed evaluation of the fate of the charge-separated state, that is, evaluation of the charge-recombination dynamics as a function of the donor-acceptor separation. An example of the decay profiles is given in Figure 5. Interestingly, extending the linkage length leads to a stabilization of the charge-separated states, despite some structural flexibility. The lifetimes, on the other hand, in the exTTF-containing nanoconjugates (**4a**: 160 ns; **4b**: 275 ns; **4c**: 335 ns) are appreciably extended relative to the analogous TTF nanoconjugates (**3a**: 190 ns; **3b**: 230 ns).

Two energy levels are important when considering the absorption of photons in SWNTs: the one that relates to free carrier thresholds, that is, free electron/hole pair continuum, and the one that relates to exciton thresholds, that is, strongly correlated electron-hole pairs (see the Supporting Information).<sup>[14]</sup> When photons that are equal to or greater in energy than the band gap are absorbed the elementary excitation is strongly excitonic in nature, based on the fairly high exciton binding energies (Coulomb interactions). It is implicit that the spatial separation is tunable by many means. Secondary

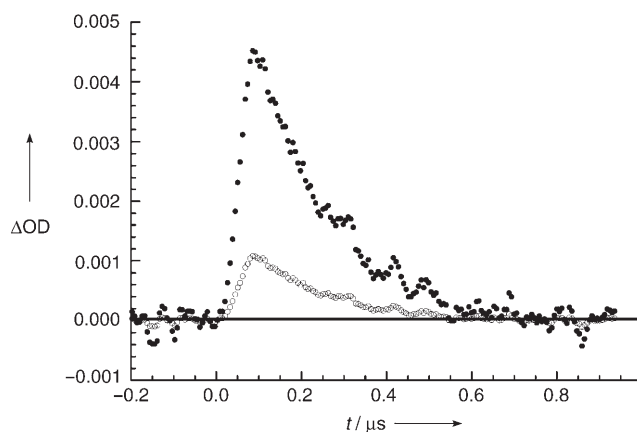


**Figure 5.** Time absorption profiles of the decay of the radical ion pairs of **4c** at 660 nm (filled circles: oxidized exTTF) and 1060 nm (open circles: reduced SWNT).

processes can, however, still afford the free electron/hole pair continuum. Alternatively, nonradiative processes from the lower lying exciton threshold are likely to populate longer-lived trap states. However, the important question about the nature of the precursor of the radical ion pair state still remains to be properly assessed.

In conclusion, time-resolved spectroscopy has helped to identify reduced SWNT and oxidized TTF and/or exTTF as metastable states in a series of donor-acceptor nanoconjugates. Overall, remarkable lifetimes in the range of hundreds of nanoseconds have been noted. Most importantly, we have succeeded for the first time in controlling the rate of electron transfer, namely, charge separation and charge recombination, by either systematically altering the relative donor-acceptor separations (**4a** versus **4b** versus **4c**) or by integrating different electron donors (**3** versus **4**).

Received: December 7, 2005

Revised: March 29, 2006

Published online: June 12, 2006

**Keywords:** charge separation · donor-acceptor systems · electron transfer · nanotubes · tetrathiafulvalenes

- [1] a) *Carbon Nanotubes: Synthesis, Structure, Properties and Applications* (Eds.: M. S. Dresselhaus, G. Dresselhaus, P. Avouris), Springer, Berlin, **2001**; b) S. Reich, C. Thomsen, J. Maultzsch, *Carbon Nanotubes: Basic Concepts and Physical Properties*, Wiley-VCH, Weinheim, **2004**.
- [2] For recent reviews, see: a) H. Imahori, *J. Phys. Chem. B* **2004**, *108*, 6130–6143; b) L. Sánchez, N. Martín, D. M. Guldi, *Angew. Chem.* **2005**, *117*, 5508–5516; *Angew. Chem. Int. Ed.* **2005**, *44*, 5374–5382; c) J. L. Segura, N. Martín, D. M. Guldi, *Chem. Soc. Rev.* **2005**, *34*, 31–47; d) L. Sánchez, M. A. Herranz, N. Martín, *J. Mater. Chem.* **2005**, *15*, 1409–1421.
- [3] For representative examples, see: a) L. W. Qu, R. B. Martin, W. J. Huang, K. F. Fu, D. Zweifel, Y. Lin, Y.-P. Sun, C. E. Bunker, B. A. Harruff, J. R. Gord, L. F. Allard, *J. Chem. Phys.* **2002**, *117*, 8089–8094; b) N. Nakashima, Y. Tomonari, H. Murakami, *Chem. Lett.* **2002**, 638–639; c) M. Alvaro, P. Atienzar, P. de la Cruz, J. L. Delgado, H. García, F. Langa, *J. Phys. Chem.*

- B* **2004**, *108*, 12691–12697; d) H. Li, R. B. Martin, B. A. Harruff, R. A. Carino, L. F. Allard, Y.-P. Sun, *Adv. Mater.* **2004**, *16*, 896–900; e) D. Baskaran, J. W. Mays, X. P. Zhang, M. S. Bratcher, *J. Am. Chem. Soc.* **2005**, *127*, 6916–6917.
- [4] D. M. Guldi, M. Marcaccio, D. Paolucci, F. Paolucci, N. Tagmatarchis, D. Tasis, E. Vázquez, M. Prato, *Angew. Chem.* **2003**, *115*, 4338–4341; *Angew. Chem. Int. Ed.* **2003**, *42*, 4206–4209.
- [5] See our studies on fullerene-based systems: a) N. Martín, L. Sánchez, D. M. Guldi, *Chem. Commun.* **2000**, 113–114; b) M. A. Herranz, N. Martín, J. Ramey, D. M. Guldi, *Chem. Commun.* **2002**, 2968–2969; c) L. Sánchez, I. Pérez, N. Martín, D. M. Guldi, *Chem. Eur. J.* **2003**, *9*, 2457–2468; d) M. Segura, L. Sánchez, J. de Mendoza, N. Martín, D. M. Guldi, *J. Am. Chem. Soc.* **2003**, *125*, 15093–15100; e) F. Giacalone, J. L. Segura, N. Martín, D. M. Guldi, *J. Am. Chem. Soc.* **2004**, *126*, 5340–5341; f) F. Giacalone, N. Martín, J. Ramey, D. M. Guldi, *Chem. Eur. J.* **2005**, *11*, 4819–4834, and references therein.
- [6] a) J. Liu, A. G. Rinzler, H. Dai, J. H. Hafner, R. K. Bradley, P. J. Boul, A. Lu, T. Iverson, K. Shelimov, C. B. Huffman, F. Rodriguez-Marcias, Y.-S. Shon, T. R. Lee, D. T. Colbert, R. E. Smalley, *Science*, **1998**, *280*, 1253–1256; b) K. J. Ziegler, Z. Gu, H. Peng, E. L. Flor, R. H. Hauge, R. E. Smalley, *J. Am. Chem. Soc.* **2005**, *127*, 1541–1547.
- [7] J. Garín, J. Orduna, S. Uriel, A. J. Moore, M. R. Bryce, S. Wegener, D. S. Yufit, A. K. J. Howard, *Synthesis* **1994**, 489–493.
- [8] a) See the Supporting Information for the synthesis and full characterization of compound **2a**; b) for the preparation of **2b** see: S. González, N. Martín, D. M. Guldi, *J. Org. Chem.* **2003**, *68*, 779–791.
- [9] a) Compound **1b** was prepared following a modified procedure by: A. Kanibolotsky, S. Roquet, M. Cariou, P. Leriche, C.-O. Turrin, R. de Bettignies, A.-M. Caminade, J.-P. Majoral, V. Khodorkovsky, A. Gorgues, *Org. Lett.* **2004**, *6*, 2109–2112; b) see the Supporting Information for the synthesis and full characterization of **2c**.
- [10] M. Prato, M. Meneghetti, unpublished data.
- [11] U. J. Kim, C. A. Furtado, X. Liu, G. Chen, P. C. Eklund, *J. Am. Chem. Soc.* **2005**, *127*, 15437–15445.
- [12] M. Melle-Franco, M. Marcaccio, D. Paolucci, F. Paolucci, V. Georgakilas, D. M. Guldi, M. Prato, F. Zerbetto, *J. Am. Chem. Soc.* **2003**, *125*, 1646–1647.
- [13] For donor–acceptor SWNT ensembles preserving the electronic structure of SWNT, see for example: a) D. M. Guldi, G. M. A. Rahman, N. Jux, N. Tagmatarchis, M. Prato, *Angew. Chem.* **2004**, *116*, 5642–5646; *Angew. Chem. Int. Ed.* **2004**, *43*, 5526–5530; b) D. M. Guldi, G. M. A. Rahman, M. Prato, N. Jux, Sh. Qin, W. Ford, *Angew. Chem.* **2005**, *117*, 2051–2054; *Angew. Chem. Int. Ed.* **2005**, *44*, 2015–2018; c) D. M. Guldi, H. Taieb, G. M. A. Rahman, N. Tagmatarchis, M. Prato, *Adv. Mater.* **2005**, *17*, 871–875; d) D. M. Guldi, G. M. A. Rahman, N. Jux, D. Balbinot, U. Hartnagel, N. Tagmatarchis, M. Prato, *J. Am. Chem. Soc.* **2005**, *127*, 9830–9838.
- [14] a) C. S. Sheng, Z. V. Vardeny, A. B. Dalton, R. H. Baughman, *Synth. Met.* **2005**, *155*, 254–257; b) A. Hagen, M. Steiner, M. R. Raschke, C. Lienau, T. Hertel, H. Qian, A. J. Meixner, A. Hartschuh, *Phys. Rev. Lett.* **2005**, *95*, 197401; c) F. Wang, G. Dukovic, L. E. Brus, T. F. Heinz, *Science* **2005**, *308*, 838–841; d) Y. Z. Ma, L. Valkunas, S. M. Bachilo, G. R. Fleming, *J. Phys. Chem. B* **2005**, *109*, 15671–15674; e) F. Wang, G. Dukovic, L. E. Brus, T. F. Heinz, *Phys. Rev. Lett.* **2004**, *92*, 177401.
- [15] D. M. Guldi, L. Sanchez, N. Martín, *J. Phys. Chem. B* **2001**, *105*, 7139–7144.
- [16] D. M. Guldi, G. M. A. Rahman, V. Sgobba, N. A. Kotov, D. Bonifazi, M. Prato, *J. Am. Chem. Soc.* **2006**, *128*, 2315–2323.
- [17] The fact that the transient features on the nanosecond time scale are instantaneous rules out any intermolecular processes.